Prediction of Gas Consumption During Hydrate Formation With or Without the Presence of Inhibitors in a Batch System Using the Esmaeilzadeh-Roshanfekr Equation of State

M. R. Talaghat,* F. Esmaeilzadeh, and J. Fathikalajahi
Chemical and Petroleum Engineering Department,
Shiraz University, Shiraz – Iran

Original scientific paper
Received: May 21, 2008
Accepted: March 30, 2009

In this work, the ability of different equations of state to predict the gas consumption during hydrate formation in a batch system has been evaluated using the model of Kashchiev and Firoozabadi. The first state equation used for this purpose was the one developed by Esmaeilzadeh and Roshanfekr. The predictions were then extended using PR, SRK and Patel Teja equations. The ability of the different equations of state were evaluated for single gases of methane and ethane and their mixtures adding to more than a thousand experimental data existing in the literature. The consumption of gas during hydrate formation was predicted both with and without the presence of kinetic inhibitors. In the case of double hydrate formation, the state equation based on the Kashchiev and Firoozabadi model for simple gas was modified by lumping the component of hydrate formation as a pseudocomponent. The results of this extension study show that the equation developed by Esmaeilzadeh and Roshanfekr is just as suitable for predicting gas consumption during hydrate formation as any of the other well known state equations such as PR and SRK.

Key words:
Gas consumption rate, equation of state, Kashchiev and Firoozabadi model, simple gas hydrate, double gas hydrate, driving force

Introduction

Gas hydrates, or clathrate hydrates, are ice-like crystalline compounds formed by the inclusion of low molecular diameter non-polar or slightly polar molecules (usually gases) inside cavities formed by water molecules. Although clathrates have similar properties to ice, they differ in that they can form at temperatures well above the freezing point of water at elevated pressure conditions. They crystallize in three well-known structures known as structure I, II and H.[1–8] Gas hydrates are reviewed in detail by Sloan.[3] In petroleum exploration and production operations, clathrates pose a serious economic and safety concern. Hydrates can block pipelines, subsea transfer lines. A well-recognized hazard in off-shore drilling is the formation of gas hydrates in the event of a hydrocarbon flow into the wellbore from the reservoir, e.g. a kick. This could potentially block the BOP (Blow-Out Preventers) stack, kill lines and chokes, obstruct the movement of the drill string, and cause serious operational problems. Gas hydrates are generally prevented by injecting so-called thermodynamic inhibitors, such as methanol, glycol etc. However, these inhibitors may not be economical at high water cuts, in addition to many environmental and logistical issues. Hence, the industry is introducing a new family of inhibitors called Low dosage hydrate inhibitors (LDHI).[9–18] Various models have been published on the basis of the crystallization theory for the prediction of gas hydrate formation. One of the most important parameters in these models is the driving force. In order to calculate the driving force of hydrate formation (the fugacity of different components in the gas phase), corresponding thermodynamic models are required. For example, Kvamme[19] used the SRK equation of state and found that the deviations from the experimental data are in directions that are to be expected from the simplifications of the model. Sloan used the SRK[3] equation of state to calculate the driving force and predict hydrate equilibrium pressure. The results indicate that the prediction of equilibrium pressure by using the SRK equation of state is closer to the experimental data. Kashchiev *et al.*[20] used the PR equation of state to predict induction time and the gas consumption rate by using the calculation of the driving force. They found that the sharp decrease in the induction time, with increasing supersaturation, is largely due to the strong supersaturation dependence of the rate of hydrate nucleation. Englezos *et al.*[21] used the Peng and Robinson equation of state to calculate the driving

* Corresponding author: talaghat@shirazu.ac.ir

force by using the fugacity coefficient of the components in the gas phase resulting in the proposed model's capability of describing the experimental data quite well with a prediction error of less than 11.3 %. In this work, the rate of gas consumption for a pure component is calculated based on the Kashchiev and Firoozabadi model with and without the presence of kinetic inhibitors. In addition, an approach for the prediction of the gas consumption rate for multicomponent gas hydrate formation based on the Kashchiev and Firoozabadi model is developed from the correlations of simple gas hydrate formation by lumping the components of the hydrate formation as a pseudocomponent. In the proposed models we also investigated the effect of using two-parameter equations of state, the [1]SRK[22]and [2]PR[23] and three-parameter equations of state, the [3]ER[24] and [4]PT[25] to predict the gas consumption rate by calculating the driving force from the fugacity coefficient of the components in the gas phase.

Gas consumption rate in simple gas hydrate formation

Nucleation is perhaps the most challenging step in understanding the process of crystallization of gas hydrate. The kinetics of gas hydrate crystallization is covered in a large number of studies in the literature. Recent studies, Makogon[26] and Sloan,[3] provide an extensive review on the subject. As far as the nucleation aspects of the crystallization process are concerned, a theoretical description of the rate of hydrate nucleation has been attempted only recently by Kavamme.[19] Several models have been published on the basis of the crystallization theory for the prediction of gas hydrate formation, but no one can predict the rate during hydrate formation very well because of the stochastic nature of the nucleation process. This in turn makes the prediction of the hydrate growth phase impossible. Several researchers[26–34] have measured the rate of gas hydrate formation after nucleation, that is, the hydrate growth stage. The rate of formation is typically expressed in terms of the gas consumption rate. Kashchiev and Firoozabadi[34] developed the rate of gas consumption model based on the early stage of the crystallization theory. The developed gas consumption rate for simple hydrate formation is defined as:

$$R(t) = \frac{\mathrm{d}n(t)}{\mathrm{d}t} = (b\rho_h V_s G^{3m} J/M_h)\, t^{3m} \qquad (1)$$

[1] Soave-Ridlich-Kowng
[2] Peng-Robinson
[3] Esmaeilzadeh-Roshanfekr
[4] Patel-Teja

For volume (J is in m^{-3} s^{-1}) progressive nucleation eq. (1) is applicable when the hydrate nucleation rate is time independent and the hydrate crystallites increase in size according to eq. (2) without having contacts with each other.

$$g(t) = \frac{\mathrm{d}r(t)}{\mathrm{d}(t)} = mG^m t^{m-1} \qquad (2)$$

In the following section, different terms of eq. (1) will be described. In the above equation, $R(t)$ is the rate of gas consumption for a pure component in simple gas hydrate formation, ρ_h is the hydrate density, V_s is the initial volume of the solution, M_h is the molar mass of the hydrate, t is time, b is the dimensionless shape factor defined as $b = 4\pi/3$ for spherical crystal, $b = 8$ for cubes, $b = [4\pi/3\ \psi(\theta)]$ for caps on a solid substrate with wetting angle θ ($0 \le \theta \le 180$) and $b = [\psi(\theta) + \psi(\theta_0)(\sin(\theta)/\sin(\theta_0))^3]$ for lenses at the solution/gas interface with angles θ, θ_0 characterizing hydrate/solution and hydrate/gas contacts, respectively. The function $\psi(x)$ is defined by eq. (3).[34]

$$\psi(x) = (1/4)(2 + \cos(x))(1 - \cos(x))^2 \qquad (3)$$

$r(t)$ as the crystallite growth hydrate formation is defined in eq. (4) based on the power law growth rate.

$$r(t) = (Gt)^m \qquad (4)$$

where, $m > 0$ is a number, G ($m^{1/m}\, s^{-1}$) is the growth constant, and t is time. Both m and G are obtainable by model considerations corresponding to the kinetics of crystallite growth. The function G is defined by the following equation:

$$G = \varepsilon A_h D_{ef} C_e [\exp(\Delta\mu/kT) - 1] = Q(e^{\Delta\mu/kt} - 1) \qquad (5)$$

for continuous or normal growth by transfer of hydrate building units across the crystallite/solution interface.[34–35,3] In the above equation, $\varepsilon \le 1$ is the sticking coefficient of building units to the crystallite surface, A_h is the surface of hydrate crystal, T is the temperature of the system, C_e is the equilibrium solubility of the gas component, Q is the supersaturation − independent kinetic factor, and D_{ef} is an effective diffusion coefficient characterizing the random events of transfer of hydrate building units across the crystallite/solution interface, respectively. $J(t) = J$, the nucleation rate is given by Kashchiev and Firoozabadi[20,34] and is defined as:

$$J = a\ \exp(\Delta\mu/kT)\ \exp(-4c^3 V_h^2 \sigma_{ef}^3/27\ kT\Delta\mu^2) \qquad (6)$$

where, c is the numerical shape factor and is equal to $(36\ \pi)^{1/3}$ and σ_{ef} (J m^{-2}) is an effective specific surface energy defined by

$$\sigma_{ef} = \Psi\,\sigma \tag{7}$$

where, Ψ is a number between 0 and 1 and is equal to $\Psi = (\psi(\theta))^{1/3}$ for cap-shaped hydrae nuclei on a solid substrate, and is equal to $\Psi = [\psi(\theta) + \psi(\theta_0)(\sin(\theta)/\sin(\theta_0))^3]^{1/3}$ for lens-shaped hydrate nuclei at the solution/gas interface; σ (J m^{-2}) is the specific surface energy of the hydrate/solution interface. It is expected to have the value of about 20 (mJ m^{-2}) which is approximately the value of the specific surface energy of ice in water. α is a kinetic parameter and is defined based on the mechanism of attachment of hydrate building units to the nucleus and mechanism of nucleation.[20] For heterogeneous nucleation on a solid substrate or at the solution/gas interface without a nucleation active center, the parameter of a is calculated by eq. (8):

$$a = z\,\varepsilon\,(4\pi\,c)^{1/2} V_h^{1/3} D_c C_e\,\dot{n}^{1/3}/A_W \tag{8}$$

In the above equations, $z = 0.01-1$ is the Zeldovich factor, V_h is the hydrate volume, and A_w is the surface area of a water molecule, D_c is the diffusion coefficient of gas in water calculated for the hydrate forming components using the Wilke-Chang correlation, as given in Reid *et al.*[36]

$$D_c = \frac{7.4\cdot 10^{-12}(\tau\,M_w)^{1/2}T}{\mu_w V_{m,i}^{0.6}} \tag{9}$$

where, D_c, M_w and μ_w are the diffusivity (m^2 s^{-1}), water molar mass (g mol^{-1}) and water viscosity (Pa s), respectively; T is the absolute temperature (K) and $V_{m,i}$ is the solute molar volume at its normal boiling point (cm^3 mol^{-1}); τ is the association factor of the solvent (for water $\tau = 2.6$). An average diffusion coefficient for the gas into water was obtained by normalizing the individual diffusion coefficient of the hydrate forming gas components, based on the composition of the hydrate forming gas in the natural gas mixture, $\dot{n}$ is the amount of building units constituting a nucleus calculated by the Kashchiev expression.[37]

$$\dot{n} = 8c^3 V_h^2 \sigma_{ef}^3/27\Delta\mu^3 \tag{10}$$

where, $\Delta\mu$ is the supersaturation or the driving force of hydrate formation.

LDHIs (Low dosage hydrate inhibitors) are known as kinetic inhibitors, because their fraction in the solution is so low (below $w = 1$ % of the aqueous phase) that they have no appreciable influence on the hydrate/solution/gas thermodynamic equilibrium.[20] From eq. (1) we see that when hydrate crystallization occurs by progressive nucleation, the additives may change either the nucleation (J) or the growth (b; G and m) of the hydrate phase or both, assuming that the growth exponent m in eq. (2) remains the same for both the blank and the additive-containing solution. By using the Langmuir adsorption isotherm for additive adsorption on the nucleation sites and growth sites, the stationary nucleation rate J and the growth constant G from eqs. (5) and (6) become:[20]

$$G_a = \frac{Q}{1 + k_g C_a}(e^{\Delta\mu/kT} - 1) \tag{11}$$

$$J_a = \frac{a}{1+k_n C_a}\,e^{\Delta\mu/kT}\exp(-4c^3 V_h^2 \sigma_{ef}^3/27kT\Delta\mu^2) \tag{12}$$

Then, the gas consumption rate for a pure component in the presence of kinetic inhibitors is defined as:

$$R(t) = \frac{\mathrm{d}n_s}{\mathrm{d}t} = (b\,\rho_h V_s G_a^{3m} J_a/M_h)\,t^{3m} \tag{13}$$

Here, n_s (mol) is the amount consumed, k_n (m^3) and k_g (m^3) are the adsorption constant and C_a (m^{-3}) is the concentration of additive in the solution, and J_a and G_a are the stationary nucleation rate and the growth constant in the presence of kinetic inhibitors.[20] The numerical solution for eqs. 1−13 will be possible if the driving force $\Delta\mu$ is known. Therefore, the following section describes how to calculate the driving force.

Driving force for simple and double gas hydrate formation

Hydrates formed from a single hydrate former are known as simple hydrates. Several driving forces have been used in the modeling of hydrate formation kinetics, and those most frequently used in experimental studies are related to the hydrate equilibrium curve. Mullin[38] defines the driving force for crystallization in terms of super-saturation. Spontaneous (homogeneous) nucleation will only occur in a supersaturated solution in the labile region limited by the super-solubility curve. In the meta-stable zone, spontaneous nucleation cannot occur, but growth of crystals is possible. For instance, the driving force for nucleation and growth can be defined by the super-saturation ratio. Vysniauskas and Bishnoi[28] used subcooling (sometimes also called supercooling) as the driving force for nucleation and growth. Subcooling is defined as the difference between the hydrate equilibrium temperature at the experimental pressure and the experimental temperature. Subcooling is easily determined by measuring the experimental temperature and calculating the hydrate equilibrium temperature using a thermodynamic model. Alternatively, the distance from the hydrate equilibrium curve in terms of pressure or fugacity can be used. Englezos[29] used

the difference in the fugacity of the dissolved gas and the hydrate equilibrium fugacity at the experimental temperature as the driving force in their hydrate formation model. Skovborg[39] expressed the driving force as the difference in the chemical potential of water in hydrate phase and water in liquid phase at experimental pressure and temperature. Skovborg and Rasmussen[40] used the difference in the gas mole fraction at interface and in the liquid bulk phase as the driving force. Kashchiev and Firoozabadi[20] derived a general expression using the supersaturation for the crystallization of one-component gas hydrates in aqueous solutions. The supersaturation is the driving force of the process, since it represents the difference between the chemical potentials of a hydrate building unit in the solution and in the hydrate crystal by the following reaction:

$$G + n_w(H_2O) \rightleftharpoons G\ n_w(H_2O) \tag{14}$$

One molecule of dissolved gas and n_w (hydration number) water molecules of the solution form one building unit ($G\ n_w(H_2O)$) of the hydrate crystal. The driving force was derived at isothermal and isobaric conditions. For isothermal conditions, the driving force was found to be

$$\Delta\mu = kT\ln[\varphi(p,T)p/\varphi e(p_e,T)p_e] + \Delta V_e(p - p_e) \tag{15}$$

where, k is the Boltzmann constant, p_e is the hydrate equilibrium pressure at T, and φ and φ_e are the fugacity coefficient of gas at given p and T and p_e and T, respectively, and ΔV_e is given by the following equation:

$$\Delta V_e = n_w(p_e,T)\cdot V_w(p_e,T) - V_h(p_e,T) \tag{16}$$

Here, ΔV_e is the difference between the volume of n_w water molecules in the solution and the volume of a hydrate building unit in the hydrate crystal at the equilibrium pressure, V_w is the molar volume for water. V_h can be calculated from

$$V_h = V_{cell}/n_g \tag{17}$$

where, n_g is the amount of gas per unit cell of hydrate crystal lattice and V_{cell} is the volume of the unit cell of the hydrate crystal lattice.

Also, Christiansen and Sloan[41] derived the driving force for hydrate formation on the basis of molar changes in the total Gibbs free energy of the system when hydrate crystal forms from water and gas. With the application of the isothermal path, for calculating the ΔG of hydrate formation, they obtained the following equation for a multicomponent system:

$$\Delta G^{\exp} = n_w(V_w - V_h)(p^{eq} - p^{\exp}) + RT\sum n_i \ln(f_k^{eq}/f_k^{\exp}) \tag{18}$$

$$\Delta g = \Delta G^{\exp}/n_g \tag{19}$$

where, ΔG^{exp} is the change in Gibbs free energy at operating conditions, Δg is the change in molar Gibbs free energy at operating conditions (the total changes of Gibbs free energy in the above operating path per amount of water consumed); n_i is the amount of gas, R is the universal gas constant,; f_i^{eq} and f_i^{exp} are the fugacity of component 'i' in the gas mixture at equilibrium and experimental conditions, respectively. These two parameters should be calculated with a suitable equation of state. In this study, several different EOS were used to calculate f_i^{eq} and f_i^{exp}.

Calculations of fugacity coefficient

Since van der Waals[42] authors have developed many empirical and semi-empirical cubic equations of state. Each trying to improve the calculation of physical properties of substances, some have modified the pressure attraction term,[43] some the pressure repulsive term,[44] and others both of the terms.[45] These equations have ranged in complexity from simple expressions containing two or three constants to complicated forms such as PHCT containing more than 50 constants. Thus, in many situations, the use of a simple cubic equation of state, which satisfies both accuracy and speed of computation time, is more convenient. Table 1 shows the summary of the equations of state used in this work. In order to calculate the driving force of hydrate formation by the above equation, fugacity of different components in gas phase, corresponding thermodynamic models are required.

Rate equation for gas consumption for double gas hydrate formation in the presence of kinetic inhibitors

In this work, Kashchiev and Firoozabadi's model[34] for a pure component is developed for the prediction of the gas consumption rate of binary gas hydrate formation by lumping the components of hydrate formation as a single component. The developed equation is given as:

$$R_s(t) = \frac{dn_s}{dt} = (b\ \rho_h V_s G_{as}^{3m} J_{as}/M_{hs})\, t^{3m} \tag{20}$$

In the above equations, $R_s(t)$ is the rate of gas consumption for pseudocomponent gas hydrate formation, n_s is the number of pseudocomponent moles consumed, ρ_{hs}, M_{hs}, G_{as}, and J_{as}, are the hy-

Table 1 – *Summary of the cubic equation of states used in this work*

SRK	PR	ER	PT
$p = \frac{RT}{V-b} - \frac{a}{V(V+b)}$	$p = \frac{RT}{V-b} - \frac{a}{V(V+b)+b(V-b)}$	$p = \frac{RT}{V-b} - \frac{a}{V(V+c)+c(V-c)}$	$p = \frac{RT}{V-b} - \frac{a}{V(V+c)+c(V-c)}$
$a = \Omega \frac{R^2T^2}{p}\alpha(T)$	$a = \Omega \frac{R^2T^2}{p}\alpha(T)$	$a = \Omega \frac{R^2T^2}{p}\alpha(T)$	$a = \Omega \frac{R^2T^2}{p}\alpha(T)$
$b = \Omega \frac{RT}{p}$	$b = \Omega \frac{RT}{p}$	$b = \Omega \frac{RT}{p}$	$b = \Omega \frac{RT}{p}$
$\alpha(T) = (1+m(1-T^{0.5}))^2$	$\alpha(T) = (1+m(1-T^{0.5}))^2$	$c = \Omega \frac{RT}{p}$	$c = \Omega \frac{RT}{p}$
$m = 0.480 + 1.574w - 0.176w^2$	$m = 0.3746 + 1.5423w - 0.2699w^2$	$\Omega = 2\Omega - 1 + 3\xi$	$\Omega = 1 - \xi$
$\Omega = 0.42747$	$\Omega = 0.45724$	$\Omega = 3\xi^2 + \Omega^2 + 2\Omega\Omega + 2\Omega$	$\Omega = 3\xi^2 + 3(1-2\xi)\Omega + \Omega^2 + 1 - 3\xi$
$\Omega = 0.08664$	$\Omega = 0.07780$	is the smallest positive root of the cubic: Ω	$\alpha(T) = (1+m(1-T^{0.5}))^2$
		$\Omega^3 + \left(3\xi - \frac{5}{8}\right)\Omega^2 + \left(3\xi^2 - \frac{3}{4}\xi\right)\Omega + \xi^3 - \frac{3}{8}\xi^2 = 0$	is the smallest positive root of the Ω cubic:
		$\alpha^{0.5} = (m_1 + m_2(1-T^{0.5}))$	$\Omega^3 + (2-3\xi)\Omega^2 + 3\xi^2\Omega^2 + \xi^3 = 0$
		$T' < T$ For $\xi = 0.32844388 - 0.0690264w + 0.0078711w^2$	$m = 0.452412 + 0.30932w - 0.297935w^2$
		$< 1T < T'$ For $\xi' = \xi - (\xi - Z)\cdot\left(\frac{T'-T}{T-1}\right)^2$	$\xi = 0.329032 - 0.076799w - 0.2211947w^2$
		$T' = 0.78921611 + 0.15855814w - 0.1331939759w^2$	$< 1T\ 0.9 < \xi' = \xi - 10(\xi - Z)(T - 0.9)$
		$m_1 = 0.999035009 - 0.010618422w - 0.0081744w^2$	
		$m_2 = 0.4400108 + 1.5297151w - 0.4710752752w^2$	

drate density, the molar mass of hydrate, the growth constant and the volume progressive nucleation for the pseudocomponent given by eqs. (21), (22), (23) and (26), respectively.

$$\rho_{hs} = \frac{N_w \cdot Mw_0 + \sum_j^{N_{com}} \sum_i^{N} y_{ij} v_i M_j}{N_A V_{cell}} \quad (21)$$

where, N_w is the amount of water per unit cell, N_A is the Avagadro's number, M_w and M_j are the molar mass of water and component j, respectively, y_{ij} is the cavity filling of component j in cavity i in the hydrate phase, v_i is the number of type i cavity per water molecule in the unit cell, V_{cell} is the volume of the unit cell, N is the number of cavity types in the unit cell, and N_{com} is the number of components in the hydrate phase.[3]

$$M_{hs} = \sum_J^{N_{com}} M_j x_{hj} + N_w \cdot M_w \quad (22)$$

Here, x_{hi} is the molar fraction of the hydrate phase, and M_w is the water molar mass.[3]

$$G_{as} = \varepsilon A_h D_e C_{es} [e^{\Delta\mu/kT} - 1] \quad (23)$$

In the above equation, ΔG is the supersaturation or the driving force of the hydrate formation given by eq. (18), D_e is the effective gas diffusivity pseudocomponent in water and C_{es} is the equilibrium solubility of the pseudocomponent given by the following eq. 24:[34–35,3]

$$C_{es} = \frac{\sum x_{ke}}{1 - \sum x_{ke}} \cdot \frac{\rho}{M_w} \cdot N_A \quad (24)$$

where, ρ (g m^{-3}) is water density, x_{ke} is the composition of guest molecule k in the free water phase at equilibrium condition[3] and is given by eq. (25):

$$x_{ke} = \frac{\hat{f}_{ke}}{H_{kw} \exp\left(\frac{WV_\infty}{RT}\right)} \quad (25)$$

Here, H_{kw} is the Henry's law constant,[3] f_{ke} is the fugacity component k in the mixture at the equilibrium condition, R is the universal gas constant, V_∞ is the infinite volume and W is energy density.

$$J_{as} = \frac{a_{as}}{1 + k_n C_a} e^{\frac{\Delta G}{kT}} \exp(-4c^3 V_h^3 \sigma_{ef}^3 / 27kT\Delta G^2) \quad (26)$$

Here, a_{as} is a kinetic parameter and is defined based on the mechanism of attachment of hydrate building units to the nucleus and mechanism of nucleation.[16] For heterogeneous nucleation on the solid substrate or at the solution/gas interface without a nucleation active center, the parameter of a_{as} is calculated by the following equation:

$$a_{as} = z\varepsilon(4\pi c)^{1/2} V_{hs}^{1/3} D_s C_{es} \dot{n}_s^{1/3} / A_w \quad (27)$$

Where, $z = 0.01 - 1$ is the Zeldovich factor, V_{hs} is the hydrate volume, and $\dot{n}_s$ is the amount of building units constituting a nucleus and is calculated based on the Kashchiev expression.[31]

$$\dot{n}_s = 8c^3 V_{hs}^2 \sigma_{efs}^3 / 27\Delta\mu^3 \quad (28)$$

Numerical method of solution

The numerical solutions for the prediction of gas consumption during hydrate formation with or without of the presence of inhibitors in a batch system for simple and double gas hydrate formation are almost the same. In this section, the method of gas consumption prediction for double gas hydrate formation without the presence of inhibitors is described. For this propose, after calculating the driving force by means of eq. (18) from different types of equations of state, the gas consumption rate for double hydrate formation was predicted using the eq. (20). The absolute deviation percent (AD) and average absolute deviation percent (AAD) between the calculated and experimental data taken from the literature for gas consumption were obtained by the following equations:

$$\% \text{ absolute deviation} = 100 \cdot |(\text{gas consumption}_i^{exp} - \text{gas consumption}_i^{cal.})| / \text{gas consumption}_i^{exp} \quad (29)$$

$$\text{AAD} = 100/n \, \Sigma |(\text{gas consumption}_i^{exp} - \text{gas consumption}_i^{cal.})| / \text{gas consumption}_i^{exp} \quad (30)$$

The rate of gas consumption in double gas hydrate formation is predicted by using the eq. (20). For this prediction, the parameters of the hydrate density (ρ_{hs}), the molar mass of the hydrate (M_{hs}), the growth constant (G_{as}) and the nucleation rate (J_{as}) are calculated by using the eqs. (21), (22), (23) and (26), respectively. The dimensionless shape factor $b = 4\pi/3 \; \psi(\theta)$, that the function $\psi(\theta)$ is calculated by eq. (3) with the selection or calculation of the wetting angle by the eq. (4).[20] For calculation of hydrate density, the cavity filling of component j in cavity i in the hydrate phase (y_{ji}) is calculated using the equation of 5−22C from Ref. [3]. For calculation of G_{as} and J_{as}, the driving force ($\Delta\mu$), the effective gas diffusivity in water (D_{efc}), the solubility of the pseudocomponent (C_{es}), the composition of guest molecule k in the free water phase at equilibrium condition (x_{ke}) and the kinetic parameter for

heterogeneous nucleation on a solid substrate or at the solution/gas interface are calculated using the eqs. (18), (9), (24), (25) and (27), respectively. With the application of the isothermal path and the selection of the types of equations of state, the driving force of hydrate formation is obtained by the calculation of the fugacity of component '*i*' in the gas mixture at equilibrium(f_i^{eq}) and experimental conditions (f_i^{exp}). The inhibitor concentration (C_a) is zero in eqs. (23) and (26), because the experiments are without the inhibitor.

The numerical shape factor (c) is equal to $(36\pi)^{1/3}$ and the effective specific surface energy (σ_{ef}) is calculated using the eq. (7). The specific surface energy of the hydrate/solution interface (σ) is about 20 (mJ m^{-2}) which is approximately the value of the specific surface energy of ice in water. The Zeldovich factor (z) and the sticking coefficient of building units to the crystallite surface (ε) are 0.01 and 1, respectively. The surface of hydrate crystal (A_h) in eq. (23) and the surface area of a water molecule (A_w) in eq. (27) are calculated by equations of $(9\pi V_{mh}^2/16)^{1/3}$ and $(9\pi V_{mw}^2/16)^{1/3}$, respectively. The remaining constants or parameters are given in Table 2.

Results and discussion

The rate of hydrate formation is directly proportional to gas consumption. Several models have been published on the basis of the crystallization theory for the prediction of gas hydrate formation. One of the most important parameters in these models is the driving force. Various driving forces have been used in order to correlate the experimental data with gas consumption data, such as supersaturation (ΔG), where it is defined as the difference between the Gibbs free energy of the hydrate unit in the supersaturated aqueous phase and the hydrate phase. In this work, the Kashchiev and Firoozabadi model was used to predict gas consumption in the simple and binary gas hydrate formation. For the prediction of the gas consumption rate in double gas hydrate formation, the rate equation based on the Kashchiev and Firoozabadi model for simple gas hydrate formation was developed by lumping the components of hydrate formation as a pseudocomponent. The model parameters related to hydrate formation kinetics are summarized in Table 2. Also, the Englezos *et al.*, Monfort *et al.* and Makogan *et al.* experiments were used to evaluate the above equations of state for prediction of gas consumption in simple and double hydrate formation. The experimental equipment of the Makogan group, consisted of a stationary cell without stirring, and a temperature and

Table 2 – *The model parameters related to hydrate formation kinetics*

Parameters	Equation or value
ΔG – independent kinetic factor, Q	eq. (5)
Effective surface energy, σ_{ef}	eq. (7)
Kinetic factor, a	eq. (8)
Effective diffusivity coefficient, D_e	eq. (9)
The number of building units, $\dot{n}$	eq. (10)
Driving force, ΔG	
For simple hydrate formation	eq. (15)
For double hydrate formation	eq. (18)
Hydrate density, ρ_h	eq. (21)
Molar mass of hydrate, M_h	eq. (22)
Equilibrium solubility of the gas component, C_e	eq. (24)
Cavity filling, y_{ij}	eq. (5−22 C) from Ref.[3]
Volume of water molecule, V_w	0.01 nm^3
Surface area of water molecule, A_w	0.12 nm^2
Surface energy of solution hydrate, σ	20 mJ m^{-2}
Zeldovich factor	0.01
Volume hydrate building unit, V_h	
For C1	0.216 nm^3
For C2	0.288
For mixture with sI hydrate structure unit	1.73
Number of water molecule, N_w	
for sI hydrate structure	46
for sII hydrate structure	136
Number of large cavities in sI & sII structure, respectively υ_i	6 and 8
Number of small cavities in sI & sII structure, respectively	2 and 16
Sticking coefficient, ε	1
Hydration number, n_w	
For C1	23/4
For C2	23/3
For gas mixture with sI hydrate structure unit	46/8
Adsorption constant, k_n, k_g	10^{-18} m^3
The initial volume of solution, V_s	400 cc
Wetting angle, Θ	60°
Dimensionless shape factor, b	$b = [4\pi/3\ \psi(\theta)]$
the surface of hydrate crystal, A_h	$(9\pi\ V_h^2/16)^{1/3}$
m for without inhibitor	1/2
m for with inhibitor	1/3

pressure control system, whereas, the Englezos group experimental apparatus consists of a semi-batch stirred tank reactor with a temperature and pressure control system, minicomputer for direct data acquisition of the process temperatures and pressures, and on-line calculation of gas consumption throughout the experiment, and use of differential pressure transducers with 0.2 % of the span. Experiments had 25 kPa error in the Heise pressure gauge and less than 0.08 K errors in all temperature readings. Also, the Monfort group experimental equipment consisted of a stirred reactor with variable gas liquid interface exchange area and recirculating flows, particle sizer system, and computer for controlling and collecting all temperatures and data. The results of the calculation of driving force dimensionless with or without the presence of kinetic inhibitors using the PR, SRK, ER and PT equations of state for the pure component of methane, ethane (at $T = 276$ K) and their mixture (75.01 % C1 and 24.99 % C2 at $T = 278$ K) are shown in Figs. 1, 2 and 3, respectively. In the aim of an unbiased comparison between the PR, SRK, ER and PT equations of state, van der Waals mixing rules were applied without the use of any adjustable parameters ($k_{ij} = 0$). Also, no pure component parameters were adjusted. In these figures, the solid curves depict the driving force vs. pressure. The curves were drawn with the aid of equilibrium pressures at $p = 3.4$, 0.62 and 1.65 MPa for pure methane and ethane, and their mixture hydrate formations, respectively. According to these figures, by increasing the pressure of the system, the calculated driving forces also increase. As can be seen in Figs. 2 and 3, for lower pressures up to 3 MPa, the calculated driving force dimensionless by the mentioned equations of state are, approximately, closer to each other; but for higher pressure (above 3 MPa), the calculated driving force, by using the PR and ER equations of state are for the most part, nearly accurate and better than the SRK and PT equations of state. Pure methane and ethane gas consumption in simple gas hydrate formation based on the Kashchiev and Firoozabadi model at various temperatures and pressures were calculated by using the PR, SRK, ER and PT equations of state and compared with the published experimental data. For this purpose, 546 experimental gas-consumption data points in simple gas hydrate formation without the presence of kinetic inhibitors from the available literature were selected. For example, the time dependence of the number of moles for crystallization of methane hydrate (at $p = 7$ MPa and $T = 276$ K) and ethane hydrate (at $p = 1.79$ MPa and $T = 276$ K) for various types of equations of state are displayed in Figs. 4 and 5, respectively. Comparison results be-

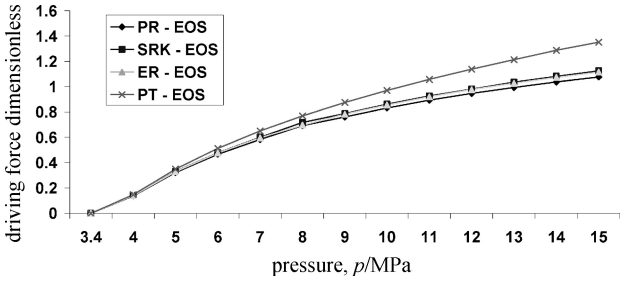

F i g . 1 – *Comparison between the calculated driving force dimensionless by various types of equations of state for methane hydrate formation with or without presence of kinetic inhibitors at T = 276 K*

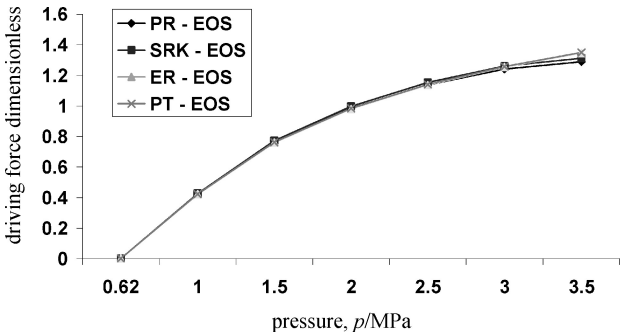

F i g . 2– *Comparison between the calculated driving force dimensionless by various types of equations of state for ethane hydrate formation with or without presence of kinetic inhibitors at T = 276 K*

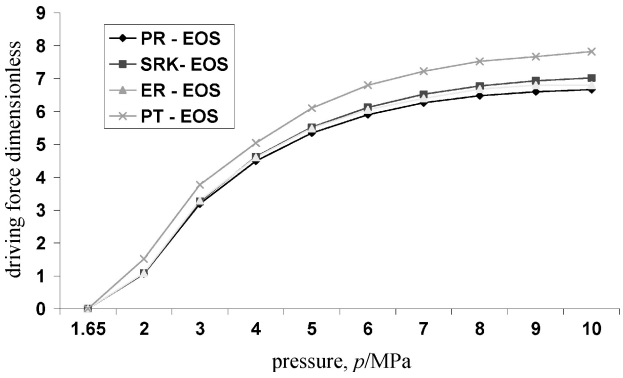

F i g 3 – *Comparison between the calculated driving force dimensionless by various types of equations of state for gaseous mixture from x = 75.01 % C1 and 24.99 % C2 hydrate formation at temperature 278 K*

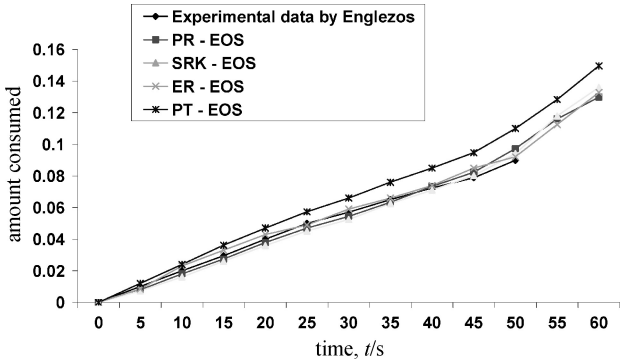

F i g . 4 – *Time dependence of the amount of methane consumed during crystallization of methane hydrate in aqueous solution at p = 7 MPa and T = 276 K for various types of equations of state*

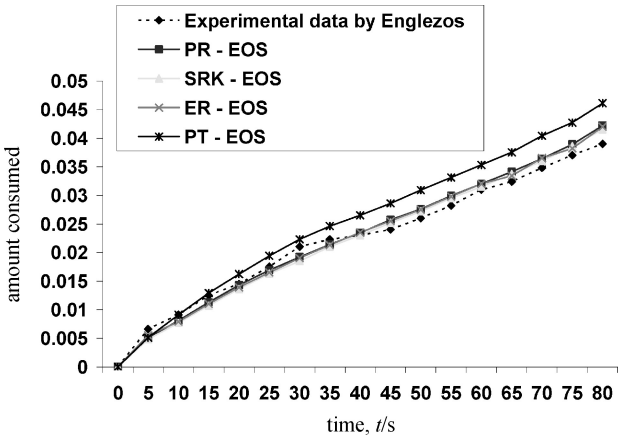

F i g . 5 – *Time dependence of the amount of ethane consumed during crystallization of ethane hydrate in aqueous solution at p = 1.79 MPa and T = 276 K for various types of equations of state*

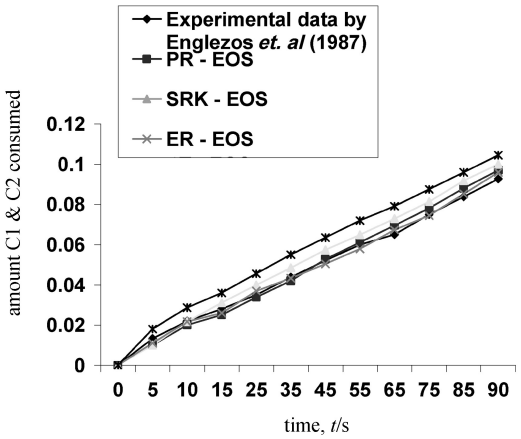

F i g . 6 – *Time dependence of the amount of gaseous mixture fraction containing x = 75.01 % C1 and 24.99 % C2 consumed during crystallization of gas mixture hydrate in aqueous solution at p = 2.58 MPa and T = 278 K for various types of equations of state*

tween the calculated and experimental published data of gas consumption indicate that the PR and ER equations of state have fewer errors than the SRK and PT equations of state for this model. The average absolute deviation between the calculated and experimental gas consumption for pure methane and ethane was also obtained. The results are shown in Table 3. In this comparison, it was found that the total average absolute deviation percentages (TAAD) of gas consumption were 7.19 %, 8.47 %, 7.20 %, and 13.92 % for the PR, SRK, ER and PT equations of state, respectively. In this work, the gas consumption for methane and ethane gaseous mixtures in double gas hydrate formation were calculated by developing the rate equation of the Kashchiev and Firoozabadi model for different compositions, temperatures and pressures with various types of equations. The average absolute deviations between the calculated and experimental data of gas consumption for methane and ethane gaseous mixtures were also obtained. For this purpose, 505 experimental gas-consumption data points in double gas hydrate formation without the presence of kinetic inhibitors from the available literature were selected. The values for AAD are demonstrated in Table 4. The total average absolute deviation percentages of the predicted gas consumption in double gas hydrate formation were found to be 11.1 %, 13.1 %, 11.3 %, and 15.6 % for the PR, SRK, ER and PT equations of state, respectively. When comparing the AAD% of gas consumption with various types of equation of state in simple and double gas hydrate formation, it can be observed that the PR and ER equations of state have fewer errors than the SRK and PT equations of state. In this comparison, the PR and ER equations of state with 9 % and 11 % AAD in simple and double gas hydrate formation are the best equations of state for calculating the driving force in the prediction of the gas consumption rate in simple and double gas hydrate formation based on the Kashchiev and Firoozabadi model. Comparison between the calculated and experimental data of gas consumption for methane and ethane gaseous mixtures (75.01 % methane and 24.99 % ethane) at pressure of 2.58 MPa and temperature of 278 K are also shown in Fig. 6. As can be seen in this figure, the PR and ER equations of state are closer to experimental data than the SRK and PT equations of state for this model. The average absolute deviations between the calculated and experimental gas consumption for ethane and its mixtures (89.4 % C1 and 10.6 % C2) in the presence of kinetic inhibitors were also obtained. The values are demonstrated in Tables 3 and 4 for simple and double gas hydrate formation, respectively. The results show the PR and ER equations of state with AAD less than 9 % and near to 10 % in simple and double gas hydrate formation with the presence of kinetic inhibitors are the best equations of state for this purpose. In this work, the total average absolute deviation between the calculated and Englezos *et al.*, Monfort *et al.*, and Makogan *et al.* experimental gas consumption in simple, double and their sum was also obtained. The results are summarized in Table 5. As can be seen, the TAAD% of the predicted gas consumption in simple and double gas hydrate formation using Englezos *et al.* experiments were found to be 9.1 %, 10.62 %, 9.1 % and 14.7 % for the PR, SRK, ER and PT equations of state, respectively. The errors using Monfort *et al.* experiments were found to be 9 %, 10.5 %, 8.8 % and 14.7 % for the PR, SRK, ER and PT equations of state, respectively.

Table 3 – *Average absolute deviation percent between of calculated gas consumption by using various types of equation of state and experimental data in simple gas hydrate formation with or without the presence of kinetic inhibitors*

No.	Component	T K	p MPa	AADY[1] PR- EOS %	AADY[1] SRK- EOS %	AADY[1] ER- EOS %	AADY[1] PT- EOS %	No. of data	Ref.
1	methane	273.75	5.6	6.3	8.4	6.3	13.8	5	26
2	methane	276	7.0	6.9	9.9	6.9	14.9	20	30
3	methane	276	6.3	6.3	8.2	6.2	14.7	19	30
4	methane	276	5.8	6.1	8.1	6.2	14.3	20	30
5	methane	276	4.9	6.1	7.9	6.2	13.9	18	30
6	methane	276	3.7	6.1	7.8	6.2	13.8	22	30
7	methane	274	7.6	7.9	10.0	7.4	14.6	20	30
8	methane	274	6.6	7.3	9.3	7.3	14.7	18	30
9	methane	274	3.7	6.5	8.9	6.5	13.2	19	30
10	methane	274	3.5	6.5	8.4	6.5	13.2	20	30
11	methane	274	3.3	6.2	8.2	6.2	12.6	20	30
12	methane	279	6.4	8.3	9.5	8.2	14.4	19	30
13	methane	279	5.8	7.8	8.9	7.7	14.1	20	30
14	methane	279	5.9	7.8	8.0	7.7	13.9	20	30
15	methane	282	8.9	8.4	9.7	8.2	14.1	22	30
16	methane	282	8.4	8.1	8.6	8.9	13.9	18	30
17	ethane	274	1.7	6.9	7.5	6.7	13.5	19	30
18	ethane	274	1.3	6.6	7.3	6.7	12.9	21	30
19	ethane	274	1.0	7.2	7.3	7.2	13.0	18	30
20	ethane	274	0.6	6.6	6.9	6.9	13.2	20	30
21	ethane	276	1.8	6.9	7.6	6.8	13.3	22	30
22	ethane	276	0.8	6.6	7.4	6.6	12.8	21	30
23	ethane	279	1.5	7.8	8.3	7.8	14.3	20	30
24	ethane	279	1.3	7.8	8.3	7.8	14.6	20	30
25	ethane	279	1.2	7.6	9.4	7.6	14.7	20	30
26	ethane	282	2.2	8.3	9.2	8.2	15.1	20	30
27	ethane	282	1.9	8.1	8.9	8.2	14.8	22	30
28	ethane	277	1.2	8.8	9.7	7.2	13.8	23	46
Total ADD% for experiments without inhibitor				7.2	8.5	7.2	13.9	546	-----
[2]29	ethane	277	1.2	8.7	9.7	8.9	13.9	20	46
[3]30	ethane	277	1.2	8.7	9.7	8.9	13.9	20	46
Total ADD% for experiments with inhibitor				8.7	9.7	8.9	13.9	40	

[1] AADY* = $100/n\ \Sigma|(\text{gas consumption}_i^{exp} - \text{gas consumption}_i^{cal.})|/\text{gas consumption}_i^{exp}$

[2] In presence of kinetic inhibitor (w = 0.05 %; VC 713)

[3] In presence of kinetic inhibitor (w = 0.05 %; PVP k15)

Table 4 – *Average Absolute Deviation percent between of calculated gas consumption by using various types of equation of state and experimental data in double gas (C1 and C2) hydrate formation with or without the presence of kinetic inhibitors*

No.	W_{c1} %	T K	p MPa	AADY[1] PR-EOS %	AADY[1] SRK-EOS %	AADY[1] ER-EOS %	AADY[1] PT-EOS %	No. of data	Ref.
1	75.01	278	2.6	9.9	11.5	10.2	15.2	23	29
2	75.01	278	2.0	9.8	11.2	10.0	15.4	19	29
3	89.4	273.75	5.1	10.0	12.8	10.3	16.6	25	29
4	75.01	281	3.6	9.7	11.7	9.5	15.4	20	29
5	75.01	281	3.0	9.6	11.7	9.5	15.1	22	29
6	25.02	274	1.4	11.7	14.6	11.9	15.6	24	29
7	25.02	274	1.2	11.0	14.3	12.3	15.6	23	29
8	25.02	274	1.1	11.3	14.0	11.8	14.8	22	29
9	25.02	276	1.2	11.6	14.6	12.2	16.3	18	29
10	25.02	276	1.0	10.8	13.9	11.3	14.8	25	29
11	25.02	276	0.9	11.1	12.73	11.7	15.6	23	29
12	75.01	284	5.6	12.3	14.9	12.5	16.6	22	29
13	75.01	284	4.1	10.9	13.9	11.4	15.4	21	29
14	50.18	280	3.9	12.3	14.5	12.3	16.1	20	29
15	50.18	280	2.5	11.4	12.3	11.5	15.1	23	29
16	50.18	274	2.1	11.3	12.3	11.3	15.9	22	29
17	50.18	274	1.7	11.4	12.4	11.4	15.7	24	29
18	50.18	274	1.5	11.2	12.2	11.2	15.4	23	29
19	50.18	274	0.9	11.2	12.3	11.3	15.3	20	29
20	50.18	274	0.8	11.0	11.9	10.8	15.2	21	29
21	25.02	274	2.0	12.7	14.8	12.8	16.6	22	29
22	25.02	274	1.3	11.8	13.0	11.9	15.8	21	29
23	25.02	274	0.7	10.8	13.7	10.9	15.1	22	29
TAAD% without Inhibitor				11.1	13.1	11.3	15.6	505	
[2]15	89.4	276	5.1	10.0	12.7	10.2	16.7	20	46

[1] $\text{AADY} = 100/n\ \Sigma|(\text{gas consumption}_i^{exp} - \text{gas consumption}_i^{cal.})|/\text{gas consumption}_i^{exp}$

[2] In presence of kinetic inhibitor

Table 5 – *Comparison TAAD between of calculated gas consumption by using various types of equation of state and experimental data in simple and double gas (C1 and C2) hydrate formation with or without the presence of kinetic inhibitors*

Simple gas hydrate formation					
Experimental data	No. of data points	TAAD PR – EOS %	TAAD SRK – EOS %	TAAD ER – EOS %	TAAD PT – EOS %
Englezos *et al.*	518	7.8	8.4	7.1	13.9
Makogon *et al.*	5	6.3	8.4	6.3	13.8
Manfort *et al.*	63	8.7	9.7	8.3	13.9
Double gas hydrate formation					
Experimental data	No. of data points	TAAD PR – EOS %	TAAD SRK – EOS %	TAAD ER – EOS %	TAAD PT – EOS %
Englezos *et al.*	505	11.1	13.1	11.3	15.6
Makogon *et al.*	-----	------	------	------	-----
Manfort *et al.*	20	10	12.7	10.2	16.7
Simple and double gas hydrate formation					
Experimental data	No. of data points	TAAD PR – EOS %	TAAD SRK – EOS %	TAAD ER – EOS %	TAAD PT – EOS %
Englezos *et al.*	1023	9.1	10.62	9.1	14.7
Makogon *et al.*	5	6.3	8.4	6.3	13.8
Manfort *et al.*	83	9.0	10.5	8.8	14.6

Conclusions

The objective of this work was to evaluate the ER EOS for predicting gas consumption in simple and double gas hydrate formation with or without the presence of kinetic inhibitors. For this purpose, the ER EOS was compared with the PR, SRK and PT equations of state. The rate of gas consumption prediction for double gas hydrate formation can be obtained directly by the Kashchiev and Firoozabadi model for simple gas hydrate formation by lumping the components of hydrate formation as a pseudocomponent. The results obtained for total average absolute deviations of gas consumption indicate that the PR and ER equations of state with 9 % and 11 % AAD in simple and double gas hydrate formation have the best overall accuracy, respectively.

ACKNOWLEDGMENT

The authors are grateful to Shiraz University and Iranian Gas Company for supporting this research.

List of symbols

- a – kinetic parameter for pure gas hydrate formation, $m^3\ s^{-1}$
- A – area, m^2
- B – shape factor
- C – numerical shape factor
- C_a – the concentration of additive in the solution, m^{-3}
- C_e – equilibrium solubility of the gas component, m^{-3}
- N_{com} – number of components in hydrate phase
- D_c – gas diffusivity in the aqueous solution, $m^2\ s^{-1}$
- f – fugacity, Pa $mol^{-1}\ m^3$
- G – growth constant, $m^{1/m}\ s^{-1}$
- H_{kw} – Henry's law constant, Pa $mol^{-1}\ m^3$
- $J(t)$ – nucleation rate, $m^{-3}\ s^{-1}$
- k – the Boltzmann constant, 1,380622 J K^{-1}
- k_n – adsorption constant for nucleation, m^3
- k_g – adsorption constant for growth, m^3
- M – molar mass, g mol^{-1}
- N – number of cavity types in unit cell
- N_w – number of water molecules per unit cell
- N_A – Avogadro's number, $6.022136 \cdot 10^{23}$ mol^{-1}
- n_w – amount of substance, mol^{-1}

$\dot{n}$ – amount of building units constituting a nucleus
n_w – hydration number
n_g – amount of gas per unit cell of hydrate crystal lattice, mol
n_i – amount of gas molecules, mol
p – pressure, MPa
Q – supersaturation − independent kinetic factor, m s^{-1}
R – universal gas constant, 8.31441 J mol^{-1} K^{-1}
$R(t)$ – rate of gas consumption for pure component, mol s^{-1}
T – temperature of system, K
t – time, s
V_s – initial volume of solution, m^3
V_m – volume, molar volume of gas component in normal boiling point, m^3 mol^{-1}
V_{mi} – number of type i cavity per water amount in unit cell
W – energy density, J m^{-3}
x_{ke} – the solubility of guest molecule k in free water phase at equilibrium condition
x – molar fraction
y_{ij} – cavity filling of component j in cavity i in hydrate phase
z – Zeldovich factor

Greek symbols

ρ – density, kg m^{-3}
θ – wetting angle on solid substrate for cap shaped or wetting angel at hydrate/solution Interface for lens shaped
θ_0 – wetting angle at hydrate/gas interface in lens shaped
Ψ – number between 0 and 1
ε – number ≤ 1 is the sticking coefficient of building units to the crystallite surface
σ – surface energy, J m^2
Φ – fugacity coefficient of gas at p and T
$\Delta\mu$ – supersaturation or driving force of hydrate formation, J
Δv_e – difference between the volume of n_w water molecules in the solution and the volume of a hydrate building unit in the hydrate crystal at the equilibrium pressure
ΔG – change in Gibbs free energy or supersaturation, J mol^{-1}
Δg – change in specific Gibbs free energy at operating conditions

Subscripts

a – presence of kinetic inhibitor
as – for gaseous mixture
cell – lattice unit cell
e – equilibrium
ef – effective
g – gas
h – hydrate
i, j, k – component
s – the pseudocomponent
w – water
∞ – infinite

Superscripts

eq – equilibrium condition
exp – experimental

References

1. *Arjmandi, M., Ren, S. R., Tohidi, B.,* Offshore Mediterranean Conference and Exhibition, Ravenna, Italy, March 26−28 (2003).
2. *Davidson, D. W,* Gas hydrates. In: *Frank, F.* (Ed.), Water: A Comprehensive Treatise, Vol 2, Plenum Press, New York, pp 115 − 234 (Chapter 3).
3. *Sloan, E. D.,* Clathrate Hydrates of Natural Gases. Second ed., Marcel Dekker, New York, 1998.
4. *Englezos, P.,* Industrial & Engineering Chemistry Research **32** (1993) 1251.
5. *Ripmeester, J. A.,* Annals New York Academy of Sciences **912** (2000) 1.
6. *Hammerschmidt, E. G.,* Industrial Engineering Chemistry **26** (1934) 851.
7. *Tohidi, B., Anderson, R., Masoudi, R., Arjamandi, M., Burgass, R., Yang, J.,* Russian Chemical Journal **47** (2003) 49, In Russian and English.
8. *Munck, J., Rasmussen, P.,* Chemical Engineering Science **43** (1988) 2661.
9. *Bishnoi, P., Dholabhai, P. D.,* Solutions. Fluid Phase Equilibria **83** (1993) 455.
10. *Tohidi, B., Danesh, A., Todd, A. C., Østergaard, K. K., Burgass, R. W., Anderson, R., Yang, J. H., Ren, S. R., Arjamandi, M., Reid, A., Ji, H., Masoudi, R.,* DTI IOR Seminar, London, UK, 29 June (2001).
11. *Barker, J. W., Gomez, R. K.,* Journal of Petroleum Technology **41** (1989) 297.
12. *Dholabhai, P. D., Kalogerakis, N., Bishnoi, P. R.,* Annual Meeting of the Petroleum Society of CIM, Calgary, Alberta, June 7–10, 1992.
13. *Østergaard, K. K., Tohidi, B., Danesh, A., Todd, A. C.,* Annals of the New York Academy of Sciences **912** (2000) 411.
14. *Lovell, D., Pakulski, M.,* Journal of Petroleum Technology **55** (2003) 65.
15. *Fu, B.,* Chemistry in the Oil Industry VII. Royal Society of Chemistry, ACS, Cambridge, UK, 2002, 264.
16. *Huo, Z., Lamar, M., Sannigrahi, B., Knauss, D. M., Sloan, E. D.,* Chemical Engineering Science **56** (2001) 4979.
17. *Zeng, H., Wilson, L. D., Walker, V. K., Ripmeester, J. A.,* Canadian Journal of Physics **81** (2003) 17.
18. *Marshall, C. B., Fletcher, G. L., Davies, P. L.,* Nature **429** (2004) 153.
19. *Kvamme, B.,* Annals of New York Academy of Science **715** (1994) 496.

20. *Kashchiev, D., Firoozabadi, A.,* Journal of crystal growth **241** (2002) 220.
21. *Englezos, P., Kalogerakis, N., Dholabhai, P. D., Bishnoi, P. R.,* Chemical Engineering Science **42** (1987) 2647.
22. *Soave, G.,* Chem. Eng. Sci. **72** (1972) 1197.
23. *Robinson, D. B., Peng, D. Y.,* Ind. Eng. Fun. **15** (1976) 59.
24. *Esmaeilzadeh, F., Roshanfekr, M.,* Fluid Phase Equilibria **239** (2006) 83.
25. *Patel, N. C., Teja, A. S.,* Chem. Eng. Sci. **37** (1982) 463.
26. *Makogan, Y. F.,* Hydrates of hydrocarbon, Penn Well Books, (1997).
27. *Knox, W. G., Hess, M., Jones, G. E., Jr., S.,* Chemical Engineering Progress **57** (1961) 66.
28. *Vysniauskas, A., Bishnoi, P. R.,* Chemical Engineering Science **38** (1983) 1061.
29. *Englezos, P., Kalogerakis, N., Dholabhai, P. D., Bishnoi, P. R.,* Chemical Engineering Science **42** (1987a) 2647.
30. *Englezos, P., Kalogerakis, N., Dholabhai, P. D., Bishnoi, P. R.,* Chemical Engineering Science **42** (1987b) 2659.
31. *Bourgmayer, P., Sugier, A., Behar, E.,* International Conference on Multiphase Flow, Nice. France, 1989.
32. *Skovborg, P., Rasmussen, H. J., Mohn, U.,* Chemical Engineering Science **48** (1993) 445.
33. *Gaillard, C., Monfort, J. P., Peytavy, J. L.,* Oil and Gas Science and Technology, Rev. IFF. **51** (1999) 365.
34. *Kashchiev, D., Firoozabadi, A.,* Journal of crystal growth **250** (2003) 499.
35. *Volmer, M.,* Kinetik der Phasenbildung, Steinkopff, Dresden, 1939.
36. *Reid, R. C., Prausnitz, J. M., Poling, B. E.,* The Properties of Gases and Liquids, fourth ed. McGraw-Hill, New York, 1987.
37. *Kashchiev, D.,* Nucleation, Butterworth-Heinemann, Oxford, 2000.
38. *Mullin, J. W.,* Crystallization, 3rd ed., Butterworth – Heinemann, Oxford, 1997.
39. *Skovborg, P.,* Ph.D. Thesis, Technical University of Denmark, 1993, 238.
40. *Skovborg, P., Rasmussen, P.,* Chemical Engineering Science **49** (1994) 1131.
41. *Christiansen, R. L., Sloan, E. D.,* Proceedings of the 74th GPA Annual Convention. San Antonio, TX, 15-21 March.
42. *van der Waals, J. D.,* Doctoral Dissertation, Leiden, The Netherlands, 1973.
43. *Vera, J. H., Stryjeck, R.,* Can. Chem. Eng. J. **64** (1986) 323.
44. *Starling, K., Carnahan, N. F.,* Chem. Phys. J. **51** (1969) 635.
45. *Sadus, R. J., Wei, Y.,* AICHE **46** (2000) 169.
46. *Monfort, J. P., Jussaume, L., Hafala, T. EL., Canselier, J. P.,* Annals of New York Academy of Science **912** (2000) 753.